Collision-induced electronic reorganization as the general mechanism of concerted cycloadditon reactions: Regioselectivity of Diels-Alder reactions

S. Sun

The Coulombic Lab of Computational Chemistry

U. S. A.

ssun@coulombiclab.com

Abstract—In the random reaction environment, two Diels-Alder reactants collide arbitrarily at one-point or one bonding location. These arbitrary collisions are simply evaluated using Hartree-Fock and density functional theory calculations. As the collision distance becomes shorter and shorter, electron density is reorganized or transferred between the reactants. A concerted transition state is then reached for the colliding complexes of the correct orientation. Concerted cycloadditions are driven by the collision-induced electron reorganization and governed by the Coulombic law. Conjugation hindrances as a controlling factor of regioselectivity are discussed using acrolein dimerization and the reaction between acrolein and 2,4-pentadienal. The actual concerted mechanism should be represented by two concerted pairs of electron-donating and accepting processes. When two ethylene molecules collide in the reality, the colliding complexes are confined to three energy minima of two gauche and one anti conformations relative to one partial single bond. An assumed concerted 2+2 transition state structure is located on a sharp ridge of the potential energy surface due to the fully eclipsed conformation. The stereo effect of the eclipsed conformation prevents the formation of a concerted transition state for ethylene dimerization. The secondarily important reason for the 2+2 step-wise mechanism is the difficulty of electron reorganization in a non-equivalent manner upon a collision.

1. Introduction

In some Diels-Alder reactions and 1,3-dipolar cycloadditions, one of the two new bonds is formed preferentially between two negative centers, and the other between two positive centers. This obfuscating natural phenomenon has stimulated a long-lasting debate for the last half century. A conceptual understanding of the concerted mechanism has not been reached based on the Coulombic law, the foundation of modern quantum mechanics. Firestone has been arguing severely for the mechanism of diradical intermediates[1-6] and Dewar had mechanistic conflicts in his mind.[7-10] The molecular orbital interaction theories[11,12] have been widely used for the mechanistic explanations of concerted cycloadditions.

Another way to look at the reality of cycloadditions is to take a closer look at the collisional modes between reactants based on the fundamental Coulombic law. Collisions between two linear molecules at one point in the space (one bonding location) are much more frequent and much stronger than simultaneously balanced collisions at two points (or two bonding locations). The two extreme consequences of the one-point-collision between two Diels-Alder reaction partners are a zwitterionic and a diradical intermediates. In these two cases, the step-wise electronic and spin (magnetic) reorganization and electron flow are initiated upon a one-point intermolecular collision. The step-wise cycloadditions are driven by electronic and magnetic interacting forces. The question is whether the one-point intermolecular collisions can also induce a concerted formation of two chemical bonds for a concerted cycloaddition. In order to answer this question, I wish to examine adiabatic thermodynamic states along different collisional modes in the gas phase using the Hartree-Fock theories (HFT) and density functional theories (DFT)[13-17] under the Born-Oppenheimer approximation. The collisions to be evaluated are arbitrary and unbalanced collisions, but have the correct orientation for a concerted formation of two new σ bonds. Two molecules come to close at one bonding location initially (at the very early stage along a reaction path), although the final transition state (TS) may be even synchronously concerted. These unbalanced collisions are clearly different from those balanced ones derived from the minimum energy path or internal reaction coordinate theory.[18] There are two reasons to examine the unbalanced collisions. First, the computational results along a minimum energy path provide no insight about how the Coulombic law functions in a concerted cycloaddition reaction. Secondly, the factors that can maintain an overall minimum energy path are not clear in the randomly collisional environment in the reality. If we assume a synchronously concerted TS for a gas phase Diels-Alder reaction, a synchronous state can only be approximately achieved at one time point along a collisional path.

When two molecules initially get close to each other at one bonding location, a strong repulsion develops to slow down the motion of the two molecules. The other two ends of the molecules at the second bonding location move faster, because of their momenta and because of relatively small repulsion. The same bonding distance can be approximately reached at the two bonding locations in the final TS for the colliding complex of the right orientation. This classic picture of molecular collisions must be examined, despite Fukui's claim that "it is difficult to imagine a simple classical picture" due to the complex nonclassical molecular motions.[18] A strong, arbitrary and unbalanced collision between two Diels-Alder reactants will efficiently induce structural and electronic reorganization. A simulation of this bimolecular collision process using RHF and DFT may provide an insight about how the two molecules behave in order to minimize the potential energy.

2. Computational Methods

In the following calculations, a constraint r_1 will be applied between the two atoms that make a collision at one bonding location. The potential energy can be then minimized to produce equilibrium geometries for variant constraint values. Relative to the constraint r_1, only one of the two gauche conformers (two local energy minima) can make a fruitful concerted reaction. The anti and the other gauche conformers are not correctly orientated for a concerted formation of two new bonds. When the distance constraint r_1 is gradually reduced (every 0.01 Å) for the gauche conformer of the correct orientation, a large number of data points can be generated. Accordingly, a large number of partially optimized structures can be obtained. We need to survey a large number of typical Diels-Alder reactions in order to get a generalized picture of the mechanism. Therefore, an intensive computational work is required. My initial attempts of the partial geometry optimization were unsuccessful at the hybrid B3LYP/6-31G* level using two different commercial software packages because of converge problems. I then chose the RHF/3-21G* method in the Spartan program[19] for the geometry optimizations under the constraint conditions, and rarely had the converge problems again. The most important aspect of this study is to pay attention to the factors that have the logical influence on the potential energy. Based on either the Schrödinger equation or DFT, the electron density is a critical variable factor that logically decides the overall potential energy increase of a colliding system. This factor is especially emphasized in the DFT, and will be, therefore, further evaluated using hybridized computational method B3LYP/6-31G* in the Titan program[20] after geometry calculations at the RHF/3-21G* level. It is well known that the structures optimized at these two different levels are somewhat different, but the energies are very close because the potential energy surface is very flat in the TS region.[10] The B3LYP/6-31G*//RHF/3-21G* calculations were

earlier demonstrated to successfully predict the major isomers of a number of stereoselective Diels-Alder reactions.[21, 22] The B3LYP/6-31G*//RHF/3-21G* calculations should also be able to provide some valuable data for the qualitative analysis of the electron reorganization behavior along different collisional paths of Diels-Alder reactions. Herein, I disclose the computational results of two Diels-Alder reactions.[23]

This computational strategy automatically assumes that two Diels-Alder reacting partners collide in "a silent state" without any thermal motions. That is, the thermal motions of the whole molecules have to be omitted to simplify the model. A synchronously concerted TS is only possible as the result of thermal motions in the reality, and will be bypassed in the model, as discussed later in this paper.

3. Results and Discussion

The Mulliken charge distribution for the ground state acrolein shown in **1** was calculated at the B3LYP/6-31G*//RHF/3-21G* level. The acrolein dimerization in Scheme 1[24] produces the regio isomer **2** as the only observed product. This phenomenon appears to violate the Coulombic law, as one of the two new bonds is formed between two electron-deficient centers and the other between two electron-rich centers.[25] There seems no attracting force to drive a bond formation between either of the compatible pairs of an electron-deficient center and an electron-rich center. This reaction was evaluated in the history using the Coulombic law-based Schrödinger equation.[26-28] Unfortunately, the Coulombic law has never been interpreted for the regioselectivity after those calculations.

Scheme 1
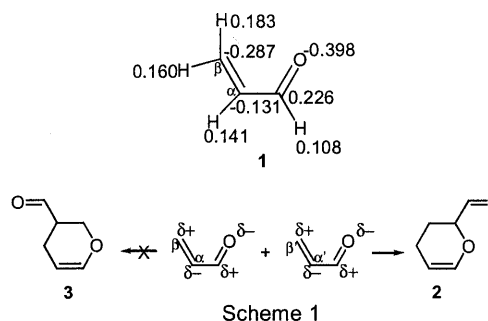
The pure HF calculations without incorporation of electron correlation could not reproduce the observed regioselectivity of this hetero Diels-Alder reaction. The fully optimized TS structures **4** ($R_{1,c-c}$=1.890 Å, $R_{2,o-c}$=2.467 Å) and **5** ($R_{1,c-c}$=2.223 Å, $R_{2,o-c}$= 1.920 Å)[23] corresponding to **2** and **3** at the B3LYP/6-31G* level have potential energy increases of 15.3 and 19.5 kcal/mol, respectively. Zero-point energy corrections are not included due to their tiny net contributions. The success of this hybridized HF-DFT method lies on the incorporation of electron correlation.

How the participating electrons move and how the Coulombic law functions in this reaction remain as questions.

The four collision modes corresponding to structures **6a-d** should eventually lead to the approximate formation of the two TS structures **4** and **5** in the actual unbalanced reaction environment. Each of the collision modes **6a-d** represents the one of the lowest potential energy among its corresponding dynamic conformers (endo/exo, dienophile-s-cis/trans). Due to the converge problems mentioned earlier, the partial geometry optimizations at the B3LYP/6-31G* level were unsuccessful under the constraint conditions, especially when the constraint is reduced to 2.0 Å or smaller. The structures corresponding to the four collision modes **a-d** were thus calculated at the RHF/3-21G* level with a graduate reduction of the collision distance r_1.[23] The resulting RHF/3-21G* structures were used for the energy calculations at the B3LYP/6-31G* level. The typical data from the calculations are summarized in Table 1. The particular structures **6a-d** were obtained at r_1=2.100 Å.
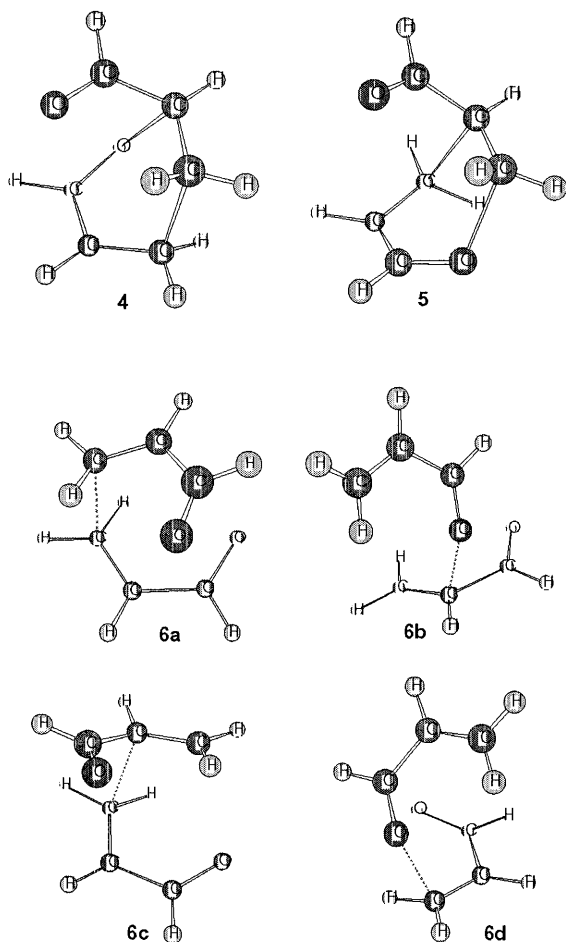

The β-β' collision **a** is between the two electrophilic β-carbon atoms. The potential energy increases moderately at the early stage of collision when $r_1 > 2.0$ Å, as compared to **b-d** (Table 1). When the collision distance r_1 is reduced to 1.85 Å, a contingency point is reached. At the contingency point, a further reduction of the collision distance by 0.01 to 1.84 Å, the second bond distance r_2 is dramatically reduced from 2.66 Å to 1.44 Å, and the potential energy drops by a sudden 25.4 kcal/mol at the B3LYP/6-31G*//RHF/3-21G* level. If r_1 were not a constraint, a concerted formation of two new single bonds could be observed. The structure at the contingency point represents the one of the highest potential energy at the 3-21G* basis level along the collision path leading to the concerted formation of the two new single bonds C-C and C-O. The highest potential energy at the B3LYP/6-31G*//RHF/3-21G* basis level is at r_1=1.88 Å. This discrepancy due to the B3LYP/6-31G* energy on the RHF/3-21G* structure is reasonable and should not affect some qualitative analysis of electron reorganization behavior. This collision process leads to the formation of **2** and has the lowest energy barrier as compared to those of the other three collision modes **b-d**.

In this β-β' collision, the two identical acrolein molecules collide in a nearly symmetrical tail-to-tail fashion. The electron reorganization during this collision path is very interesting. The Mulliken charge distribution at the B3LYP/6-31G*//RHF/3-21G* level is shown in **7a** and **7b** corresponding to r_1=2.10 and 1.85 Å.[23] The two electrophilic β positions have the strong tendency to compete for electrons with the same amount of power. The net result of the competition is the nearly equal electron sharing between the two β positions. Relative to the ground state acrolein **1**, each β-CH$_2$ group has a total Mulliken charge decrease of 0.024 and 0.023 (more negative) at r_1=2.10 (**7a**) and 1.85 Å (**7b**), respectively. Accordingly, each α-CH group has a total charge increase of 0.055 and 0.074 (more positive), respectively. The α-position of acrolein becomes electron-deficient when compared to its ground state, and can undergo an eletrophilic attack. Each carbonyl oxygen atom develops more negative charge, and its ability of nucleophilic attack is actually enhanced. In the actual reaction environment, the more synchronized TS **4** can be reached approximately. When the distance r_2 between O-α' decreases, the balanced electron sharing mentioned above between the two β-positions will be affected. The electrons are forced to move in a circular fashion as shown by **10a**. The diene oxygen atom donates while the α-carbon of dienophile accepts electron density, forming a ring current with a defined direction. The driving force for the formation of the regio isomer **2** is the Coulombic law-based electron reorganization. The actual mechanism should be described by two concerted pairs of electron-donating and accepting processes.

Table 1. Collision modes, r_1 and r_2 values (Å), and relative potential energies (kcal/mol, without zero-point energy corrections) for the unbalanced collisions of acrolein dimerization. The r_2 values for the O-β' collision (**d**) are corresponding to the product **11a**.

Mode	r_2 (r_1=2.10)	Energy	r_2 (r_1=1.90)	Energy	r_2 (r_1=1.85)	Energy	Contingency point r_1	Contingency point r_2	Energy	Product
β-β', **a**	2.956	13.40	2.728	16.26	2.616	16.11	1.850	2.616	16.11	**2**
O-α', **b**	4.361	13.38	3.649	24.86	3.460	27.45	1.730	2.904	33.72	**2**
β-α', **c**	2.670	21.19	-	-	-	-	2.050	2.503	22.54	**3**
O-β', **d**	2.899	9.32	2.639	16.43	2.500	17.81	1.830	2.380	18.11	**11a**

**7a**   **7b**   **8**   **9**

10a   **10b**   **10c**
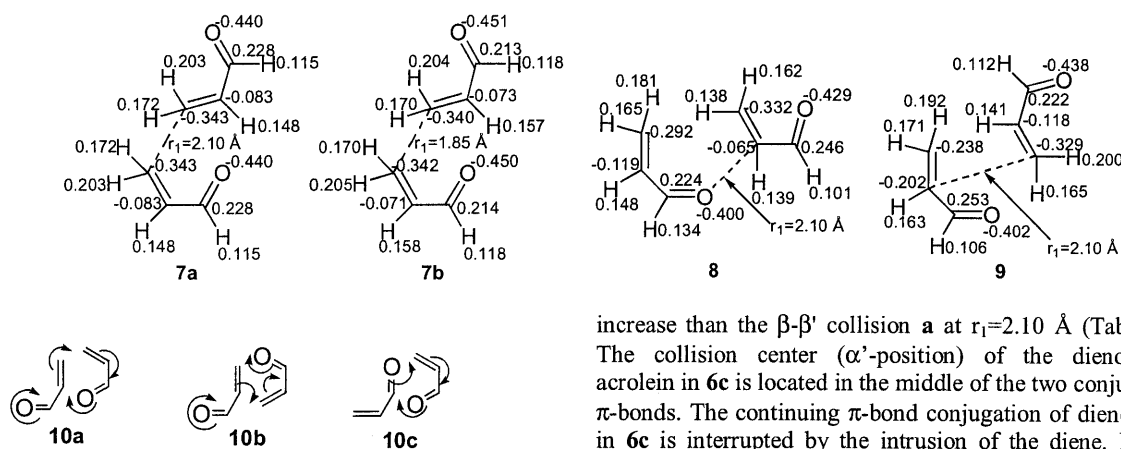
The O-α' collision mode **b** is between the diene oxygen and the α-carbon of the dienophile. The Mulliken charge distribution corresponding to **6b** (r_1=2.100 Å) is shown in **8**. The potential energy increase is smaller than that of the β-β' collision in the early collision stage ($r_1 > 2.1$ Å, Table 1). This could be partially caused by a steric effect due to the two hydrogen atoms on the β-carbon but nothing on oxygen. The increase is then sharply faster with a further progress of the collision. The final potential energy at the contingency point at r_1=1.73 Å is 33.7 kcal/mole, higher than that of the β-β' collision. The diene loses and the dienophile gains electron density via the O-α' interaction. The net charge transfer from the diene to the dienophile at r_1=2.10 Å is 0.041 as shown in **8**. The electron density is so distributed that the β' –CH$_2$ group of the dienophile becomes electron-rich with a total charge density of -0.032, while the electron density of the α' position is reduced. The β' carbon clearly evolves the ability of nucleophilic attack in the collision course. In the actual reaction environment, the same TS **4** can be reached approximately via this O-α' collision. The electrons can flow in the same manner as depicted in **10a**.

The -α' collision **c** is between the electrophilic β-carbon of the diene and the α-carbon of the dienophile. This collision has a dramatically higher potential energy

increase than the β-β' collision **a** at r_1=2.10 Å (Table 1). The collision center (α'-position) of the dienophilic acrolein in **6c** is located in the middle of the two conjugated π-bonds. The continuing π-bond conjugation of dienophile in **6c** is interrupted by the intrusion of the diene. In the other words, **6c** can be seen as to have a branched intermolecular conjugation system. In contrast, the π-bond conjugation in **6a** is linear in a tail-to-tail fashion, and is more favorably extended intermolecularly through an equal sharing of electrons between the two molecules. Such an effect leading to the potential energy difference between **6a** and **6c** may be seen as a result of conjugation hindrance in **6c**. The electron density on the α-carbon of the ground state dienophile is held tightly by the carbonyl group due to its polarization effect, and an electrophilic invasion will not be easy here. The net charge transfer is 0.044 from the dienophile to the diene via the β-α' interaction as shown in **9**, but the high energetic price must be paid. In the actual reaction environment, the collision **6c** would lead to a faster closure of the second new bond O-β', so that a TS **5** can be approximately reached. The oxygen-carbon interaction is much weaker electronically than the carbon-carbon interaction as will be discussed later. The closure of the second new bond O-β' provides a very limited release of the sharp confrontation caused by the β-α' collision. Therefore, the total potential energy increase of **5** is higher than that of **4**. The reaction mechanism can only be expressed by the electron-donating and accepting relationship as shown in **10b**.

The O-β' collision mode **d** has the lowest potential energy compared to **a-c** at r_1=2.10 Å (Table 1). This might reflect the effect of the attraction between the positive β'-CH$_2$

group and the negative oxygen atom. As r_1 is further reduced, the potential energy increases faster, and becomes higher than that of the collision path **a** at $r_1=1.90$ Å (Table 1). Interestingly, the second bond distance between β-α' positions leading to the formation of **3** becomes larger as r_1 becomes smaller. At $r_1=1.83$ Å, a contingency point is reached so that a further reduction of r_1 by 0.01 Å between the O and β'-C atoms, a second bond is formed. This second bond is corresponding to the product **11a**. That is, the carbonyl group (C=O bond) is an active dienophile in this O-β' collision. I searched all possible conformers at both AM1 and the RHF/3-21G* basis levels based on this O-β' collision mode at a constraint of 2.10 Å. But a path was not found that can lead to the formation of **3**. The four TS structures (s-cis/trans, endo/exo) for the isomer **11a** were calculated at the B3LYP/6-31G* level. Among them, the cis/endo structure **11b** has the lowest relative potential energy of 17.54 kcal/mol. The relative potential energy of **11b** is lower than that of **5** (19.54 kcal/mol), but higher than that of **4** (15.28 kcal/mol) without zero point energy corrections due to their very small net contributions. Therefore, the potential energies along different modes of the unbalanced collision may qualitatively reflect the easiness for a particular isomer to be formed. The circular electron flow for the formation of **11a** is shown in **10c**, a mechanism of two concerted pairs of electron-donating and accepting processes.

11a

11b
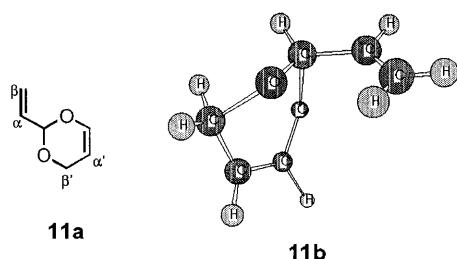
The resisting force is smaller in the initial stage of an O-C collision path, and increases sharply as the collision develops further ($r_1 < 2.0$ Å). The electronic interaction is significantly less favored with the stronger resistance at a shorter O-C constraint, even though the colliding centers are a compatible negative-positive pair such as that in **6d**. This phenomenon can be easily understood based on the incompatibility between a hard nucleophilic oxygen atom (a hard base) and a soft electrophilic carbon atom (a soft acid) in the conventional chemistry.[29] This hard-soft incompatibility can be seen as a second type of conjugation hindrance, and appears to relate closely to the electronic correlation in the quantum mechanic calculations.

The second example is the Diels-Alder reaction between acrolein and 2,4-pentadienal (Scheme 2). This Diels-Alder reaction is a simplified model for the observed Diels-Alder reaction between acrylic acid and 2,4-pentadienoic acid.[30, 31] When one of the two new bonds is formed between the

two electron-deficient centers (β and δ') and the other is between the two electron-rich centers (α and α'), the major regio isomer **12a** is formed. When each of the two new bonds is formed between a compatible pair of rich-deficient centers (β-α' or δ'-α), the minor isomer **12b** is formed. This reaction cannot be clearly understood without applying the fundamental concepts included in the Schrödinger equation.
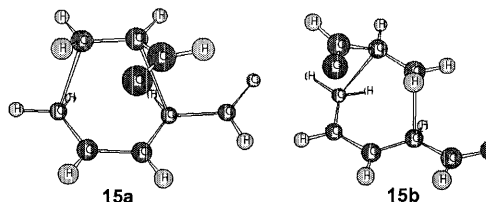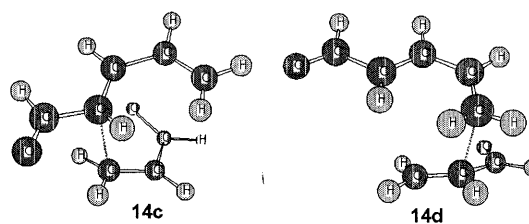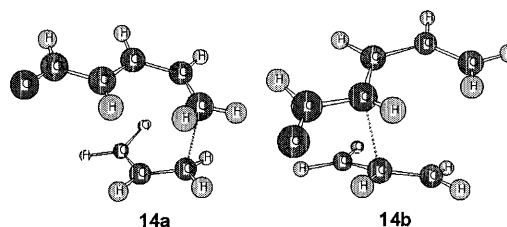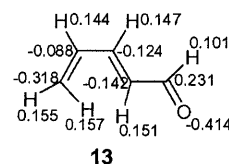
Scheme 2

12a, Major   **12b**, Minor

13

14a   **14b**

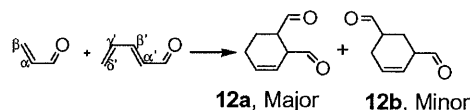**14c**   **14d**

15a   **15b**

Table 2. Collision modes, r_1 and r_2 values (Å), and relative potential energies (kcal/mol, without zero-point energy corrections) for the unbalanced collisions between acrolein and 2,4-pentadienal.

Mode	r_2 (r_1=2.10)	Energy	Contingency point r_1	Contingency point r_2	Energy	Product
β-δ', **14a**	3.186	13.00	1.960	2.840	13.99	**12a**
α-α', **14b**	2.955	24.00	2.050	2.751	25.49	**12a**
β-α', **14c**	3.172	16.39	1.960	2.907	18.88	**12b**
α-δ', **14d**	3.139	21.07	2.060	2.906	21.97	**12b**

16a   **16b**   **16c**   **16d**
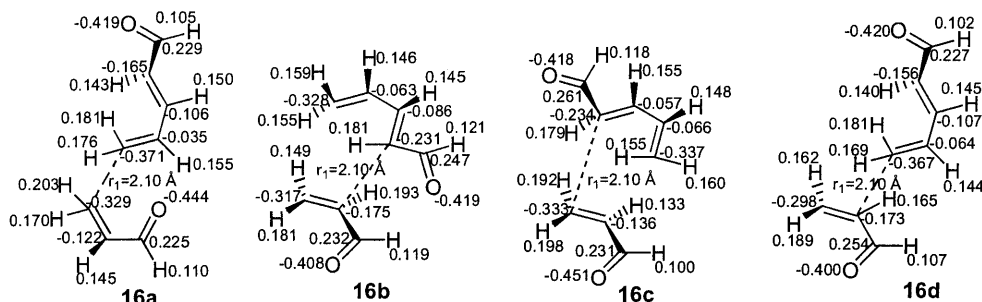
The Mulliken charge distribution of ground state pentadienal is shown in **13** as calculated at the B3LYP/6-31G*//RHF/3-21G* level. The four possible collision modes **14a-d** should eventually lead to the approximate formation of the two TS structures **15a** and **15b** in the actual unbalanced reaction environment. The Mulliken charge distributions corresponding to the four collision modes (**14a-d**) at the collision distance r_1=2.10 Å are shown in **16a-d**, as calculated at the B3LYP/6-31G*//RHF/3-21G* level. The relative potential energies are listed in Table 2. The fully optimized TS **15a** has a relative potential energy of 14.09 kcal/mol at the B3LYP/6-31G*//RHF/3-21G* level, and two partial single bond lengths of 2.050 Å (β-δ') and 2.362 Å (α-α'). The TS **15b** has a relative energy of 16.39 kcal/mol, and two partial single bond lengths of 2.125 Å (β-α') and 2.276 Å (α-δ'). Zero-point energy corrections are not considered.

The β-δ' collision **14a** has the lowest potential energy among all the four collision modes (Table 2). The electron transfer from 2,4-pentadienal to acrolein is 0.042 at r_1=2.10 Å as shown in **16a**. The aldehyde substituent CHO of acrolein captures essentially all the electron gain and has a total electron density increase of 0.045. The charge density redistribution upon the collision generates a reorganized electric field between the two reactants. Such an initial collision changed the fundamental electron-rich and electron-deficient relationship between the two reactants. The diene becomes electron-deficient while the dienophilic acrolein becomes electron-rich. As the second partial bond length r_2 is reduced due to the thermal motions in the

reality, an electron flow is forced from the electron-rich acrolein to the electron-deficient pentadienal via the partial bond r_2. Such an electron flow can not be simply understood based on the charge densities of two individual α-carbon atoms. Compared to the ground state **13**, the electron density is largely reduced at the β' and γ' positions in **16a**. The β' and γ' positions have the power to compete for electron density, so that the electron density can shift over from the α'-position as r_2 decreases. The other side of the α' position of pentadienal is the electron deficient CHO group, which also has the strong power to compete for electron density. Overall, the participating electrons can flow as shown in **17a**. The arrow of half circle on the oxygen atom in **17a** is assigned here to represent the electron enrichment in the middle of the reaction path. This is a mechanism of two concerted pairs of electron-donating and accepting processes. The α'-position in pentadienal accepts electron density while the α-position of acrolein donates electron density, as driven by collision-induced electronic redistribution. Further evidence for the electron flow **17a** will be discussed later based on a tetramer complex structure **18a**.

17a   **17b**   **17c**   **17d**
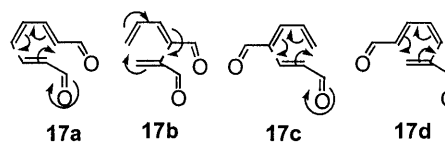
The conjugation hindrance is seen in the collision modes **14b-d**. The electron transfer for the α-α' collision **14b** (r_1=2.10 Å) is 0.026 from pentadienal to acrolein. This collision mode encounters a high resistance in the early collisional stage (Table 2). Further calculational data indicate that the assumed electron flow **17b** can not take place as r_2 decreases, as mentioned later based on **18b**. The collision paths **14c-d** share the similar electron flow direction shown in **17c-d**, because the initial electron transfer is from diene to dienophile for **14c**, and is from dienophile to diene for **14d**. More detailed analyses of these two colliding paths **14c-d** would be omitted here.

The remaining question is whether the collision mode **14a** can really induce a circular electron flow **17a**. Can we get any direct or indirect evidence of the ring current? As r_2 decreases, the potential energy will continue to increase until the TS is reached. At the TS, the potential energy will start to fall. What is the kinetic reason for the fall of potential energy based on a well-known law of physics? The fall of potential energy could be achieved via a mechanism of a spontaneous ring current. This would imply that the circular electron flow would take place gradually after the TS in a reaction path. We are certainly blinded about what is really going on if we just look at the TS structure or just look at any structures along a minimum energy path. But the unbalanced collision structure **14a** could give us a hint. The electron transfer across r_2 partial bond can be visualized in an intermolecular-like fashion. That is, we can connect two unbalanced colliding systems and examine the trend of possible electronic flow.

Two β-δ' colliding systems connected by a constraint r_3 is shown in **18a**. The first colliding system consists of Ene1 and Diene1 with a constraint r_1, and the second colliding

system consists of Ene2 and Diene2 with a constraint r_1'. The constraint r_3 is between α-carbon of Ene2 and α'-carbon of Diene1. This tetramer complex structure of three constraints (r_1, r_1' and r_3) was calculated at the RHF/3-21G* level. The Mulliken charges at the B3LYP/6-31G*//RHF/3-21G* level are given in **18a** with $r_1 = r_1' = r_3 = 2.0$ Å. The three arrows on the right in **18a** represent the directions of electron flow across the constraints, and the numbers next to the arrows are the amounts of electron transfer. In Table 3, the quantities of electron transfer calculated under different constraint values are given corresponding to the same flow directions shown in **8a**. These quantities increase significantly as the partial bond lengths decrease. The electron transfer across r_3 is close to zero when the constraint values are close to the partial bond lengths of the TS structure. This should be understandable because of the zero force state across the new partial bonds at the real TS. This can be imagined to be a ball that just starts to roll down with a zero speed from the top of a mountain.

Table 3. Quantities of electron transferred across r_1, r_1' and r_3 under different constraint values corresponding to structure **8a**.

Constraint values (Å) $r_1 = r_1' = r_3 =$	Electron transfer at r_1	Electron transfer at r_3	Electron transfer at r_1'
2.10	0.066	0.004	0.013
2.05	0.081	0.018	0.014
2.00	0.097	0.031	0.016
1.95	0.127	0.069	0.039

In this open chain system **18a**, charges are built up in the two terminals, and the potential energy continues to increase as the constraint values decrease. In a closed ring

18a

18b
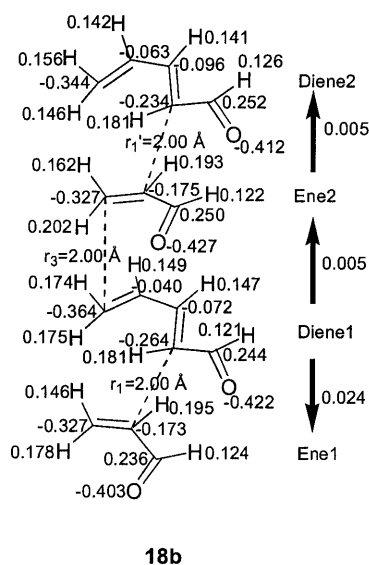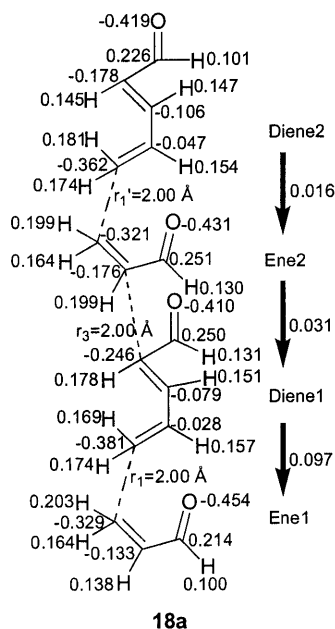
system such as **15a**, charges can not be built up due to the constant charge neutralization as the reaction proceeds, and the potential energy falls as the electrons move spontaneously. The actual amounts of electron transfer could be an order larger in a closed ring circuit than in **18a**. This model study provides us sufficient evidence that the electron flow in **17a** from the α position of acrolein to the α' position of 2,4-pentadienal can take place in the reality.

In Structure **18b**, electron flows so easily from the α position of Ene2 to the α' position of Diene2 *once* there is a tiny electron supply to the β position of the Ene2. Structures **18a** and **18b** show that the electron can not flow from the β position of acrolein to the δ' position of pentadienal after TS whatever, but can always flow from the δ' position of pentadienal to the β position of acrolein regardless of collisional paths. As the β-δ' distance (r_2) decreases in the progress of the α-α' collision mode **14b**, electron will flow from the δ' position to the β position. The electron flow from the α' position to the α position at the very early collisional stage will be reversed as the collision progresses in the reality. Therefore, **14b** can not induce electron-flow pattern **17b**, but will eventually lead to the same electron flow shown in **17a**. In the reality, an electron supply to the β position of acrolein exist because the β-δ' partial bond is shorter than α-α' partial bond in the TS **15a**. The electronic flow in structure **17a** applies not only to the collisional modes **16a** and **16b**, but any collisional mode between these two extremes including the minimum energy path.

The electronic reorganization based on the Coulombic law during a molecular collision is a logical consequence, and is a ubiquitous natural phenomenon that can not be avoided. π-Bond electrons are relatively soft and flexible. When two molecules containing π-electrons get close, they polarize each other. Due to the strong spin coupling of electron pairs in closed shell systems, the spin-based magnetic interacting force is less active than Coulombic forces. To my point of view, those existing arguments for diradical intermediates or for concerted spin coupling processes[26b,32] are indirect. I would think that spin polarization is mandatory in the early stage of collisions (prior to TS) for the magnetic force as the controlling power. A direct demonstration of the spin polarization using spin populations in unbalanced collisions is yet to be done. The intrinsic kinetic driving force is covered up along the minimum energy paths. Therefore, there is still a long way to go for an eventual confirmation of the real power (magnetic or Coulombic force) that controls the cycloaddition reactions. In this current paper, it is demonstrated that the regioselectivity of Diels-Alder reactions can be well explained simply according to the Coloumbic law and conjugation hindrances.

When two ethylene molecules collide in the reality, the colliding complex is confined to three energy minima of two gauche and one anti conformations relative to one partial single bond. These three conformers are distorted too much from any possible concerted TS. In the other words, possible concerted thermodynamic states towards an assumed concerted 2+2 TS structure are located on a sharp ridge of the potential energy surface. The fundamental reason for the step-wise mechanism is the stereo effect due to the bond-bond repulsion of the eclipsed conformation. This "geometrically difficult transition state" has been well recognized earlier.[33] The secondarily important reason for the step-wise mechanism is the difficulty of electron reorganization in a non-equivalent manner upon a collision. In contrast, a Diels-Alder reaction has the fundamental advantage of the local energy minimum of a gauche conformation that can lead to the formation of concerted TSs. Diels-Alder reacting partners are two non-equivalent molecules and can induce non-equivalent electron redistribution upon a collision.

In some cases that the bond-bond repulsion of the eclipsed conformation can be significantly reduced via a facile electronic reorganization, concerted 2+2 cycloadditions do take place.[34,35] The one between sulfur trioxide and ethylene has been well calculated in Houk's group.[34] They contributed this unusual 2+2 reactivity to the *polar* TS. It is evident that the polar TS is the result of electron reorganization when the reactants come to close to each other. When a concerted bond forming process involves hetero atoms such as those in sulfur trioxide, the electron reorganization can be more easily seen due to the uneven charge distribution. After all, the fundamental laws governing the 2+2 and Diels-Alder reactions remain unchanged, and should be understood in any explanations of the concerted mechanism.

4. Conclusion

Chemical reactions including the concerted cycloadditions can not be understood without clarifying the intrinsic kinetic driving forces and hindrances. Dissecting the concerted TS structures of cycloaddition reactions may provide us an opportunity to reveal how those fundamental laws of physics operate. A dissection has been approached in this paper by modeling one-point unbalanced collisions. The computational results of one-point unbalanced collisions indicate that electronic reorganization can efficiently shape the concerted TS structures of Diels-Alder reactions. The major product of a concerted cycloaddition should derived from a one-point unbalanced collision that can maximize the intermolecular conjugation (or delocalization) effect. The conjugation hindrances impair the intermolecular conjugation effect, and inhibit the kinetic motions of participating electrons in the corresponding collision paths. Due to the conjugation hindrances, new chemical bonds can not be favorably formed sometimes between the compatible pairs of positive-negative centers. One of the two new bonds can be

preferentially formed between two negative centers and the other between two positive centers in many concerted cycloaddition reactions. This is because the electrons can redistribute efficiently based on the Coulombic law upon the corresponding collision. The similar electronic reorganization based on the Coulombic law will be reported in due course for the parent Diels-Alder reaction, 1,3-dipolar cycloadditions, and concerted 2+2 reactions.

5. References

1. Firestone, R. A. *J. Org. Chem.* **1968**, *33*, 2285.
2. Firestone, R. A. *J. Org. Chem.* **1972**, *37*, 2181.
3. Firestone, R. A. *Tetrahedron* **1977**, *33*, 3009.
4. Firestone, R. A. *J. Org. Chem.* **1976**, *41*, 403.
5. Firestone, R. A. *Heterocycles* **1987**, *25*, 61.
6. Firestone, R. A. *Tetrahedron* **1996**, *52*, 14459.
7. Dewar, M. J.; Jie, C. *Acc. Chem Res.* **1992**, *25*, 537.
8. Dewar, M. J. S. *J. Am. Chem. Soc.* **1984**, *106*, 209.
9. Dewar, M. J. S. *THEOCHEM*, **1989**, *200*, 301.
10. Houk, K. N.; Gonzalez, J.; Li, Y. *Acc. Chem. Res.* **1995**, *28*, 81.
11. Fukui, F. *Science* **1982**, *218*, 747.
12. Woodward, R. B.; Hoffmann, R. *Angew. Chem. Int.* **1969**, *8*, 781.
13. Hohenberg, P.; Kohn, W. *Phys. Rev.* **1964**, *B136*, 864.
14. Kohn, W.; Sham, L. *J. Phys. Rev.* **1965**, *A140*, 1133.
15. Ziegler, T. *Chem. Rev.* **1991**, *1991*, 651.
16. Kohn, W.; Becke, A. D.; Parr, R. G. *J. Phys. Chem.* **1996**, *100*, 12974.
17. Baerends, E. J.; Gritsenko, O. V. *J. Phys. Chem. A* **1997**, *101*, 5383.
18. Fukui, F. *Acc. Chem. Res.* **1981**, *14*, 363.
19. PC SPARTAN pro (v. 1), Wavefunction, Inc., Irvine, CA.
20. TITAN (v. 1), Wavefunction, Inc., Irvine, CA; and Schrödinger, Inc., Portland, OR.
21. Murray, W. V.; Sun, S.; Turchi, I. J.; Brown, F. K.; Gauthier, A. D. *J. Org. Chem.* **1999**, *64*, 5930.
22. Sun, S.; Turchi, I. J.; Xu, D.; Murray, W. V. *J. Org. Chem.* **2000**, *65*, 2555.
23. r_1: Represents the partial bond length at the primary bonding or colliding location in an unbalanced collision; is the shorter partial bond in the unbalanced collision; is a constraint in the calculations; and is represented by a dotted or dashed line in the structural drawings in this paper. r_2: Represents the partial bond length at the secondary bonding or colliding location in an unbalanced collision; is the longer partial bond length in the unbalanced collision for each presumed Diels-Alder reaction; is not a constraint in the calculations so that its value is obtained from the partial geometry optimization; is blank (not drawn) in the structural drawings. R_1 and R_2 represent a pair of the partial single bond lengths of the fully optimized TS without any constraint for a particular Diels-Alder reaction.
24. The symbols δ- and δ+ represent electron rich and electron deficient positions, respectively. α, β, γ, And δ are used to number individual positions of the first reactant, and α', β', γ', and δ' are used to number those of the second reactant.
25. The α-CH of acrolein is electron-rich relative to the 2-CH of 1,3-butadiene, as a result of polarization effect of the aldehyde substituent.
26. (a) Toma, L.; Quadrelli, P.; Caramella, P. *Tetrahedron Lett.* **2001**, *42*, 731; (b) Toma, L.; Romano, S.; Quadrelli, P.; Caramella, P. *Tetrahedron Lett.* **2001**, *42*, 5077.
27. Devaquet, A.; Salem, L. *J. Am. Chem. Soc.* **1969**, *91*, 3793.
28. Desimoni, G.; Tacconi, G. *Chem. Rev.* **1975**, *75*, 651.
29. Pearson R. G. *J. Am. Chem. Soc.* **1963**, *85*, 3533.
30. Fleming, I. *Frontier Orbitals and Organic Chemical Reactions*; John Wiley & Sons: London, 1976; pp.129.
31. Fleming, I.; Michael, J. P.; Overman, L. E.; Taylor, G. F. *Tetrahedron Lett.* **1978**, 1313.
32. Karadakov, P. D.; Cooper, D. L.; Gerratt, J. *J. Am. Chem. Soc.* **1998**, *120*, 3975.
33. Houk, K. N.; Li, Y.; Evanseck, J. D. *Angew Chem. Int. Ed. Engl.* **1992**, *31*, 682.
34. Haller, J.; Beno, B. R.; Houk, K. N. *J. Am. Chem. Soc.* **1998**, *120*, 6468.
35. Salzner, U.; Bachrach, S. M. *J. Org. Chem.* **1996**, *61*, 237.